

RNA Structure and RNA–Protein Interactions in Purified Yeast U6 snRNPs

Ramazan Karaduman¹, Patrizia Fabrizio¹, Klaus Hartmuth¹
Henning Urlaub² and Reinhard Lührmann^{1*}

¹Max-Planck-Institute of
Biophysical Chemistry
Department of Cellular
Biochemistry, Am Fassberg 11
D-37077 Göttingen, Germany

²Bioanalytical Mass
Spectrometry Group, Am
Fassberg 11, D-37077 Göttingen
Germany

The U6 small nuclear RNA (snRNA) undergoes major conformational changes during the assembly of the spliceosome and catalysis of splicing. It associates with the specific protein Prp24p, and a set of seven LSm2p–8p proteins, to form the U6 small nuclear ribonucleoprotein (snRNP). These proteins have been proposed to act as RNA chaperones that stimulate pairing of U6 with U4 snRNA to form the intermolecular stem I and stem II of the U4/U6 duplex, whose formation is essential for spliceosomal function. However, the mechanism whereby Prp24p and the LSm complex facilitate U4/U6 base-pairing, as well as the exact binding site(s) of Prp24p in the native U6 snRNP, are not well understood. Here, we have investigated the secondary structure of the U6 snRNA in purified U6 snRNPs and compared it with its naked form. Using RNA structure-probing techniques, we demonstrate that within the U6 snRNP a large internal region of the U6 snRNA is unpaired and protected from chemical modification by bound Prp24p. Several of these U6 nucleotides are available for base-pairing interaction, as only their sugar backbone is contacted by Prp24p. Thus, Prp24p can present them to the U4 snRNA and facilitate formation of U4/U6 stem I. We show that the 3' stem-loop is not bound strongly by U6 proteins in native particles. However, when compared to the 3' stem-loop in the naked U6 snRNA, it has a more open conformation, which would facilitate formation of stem II with the U4 snRNA. Our data suggest that the combined association of Prp24p and the LSm complex confers upon U6 nucleotides a conformation favourable for U4/U6 base-pairing. Interestingly, we find that the open structure of the yeast U6 snRNA in native snRNPs can also be adopted by human U6 and U6atac snRNAs.

© 2006 Elsevier Ltd. All rights reserved.

Keywords: yeast U6 snRNP; yeast U6 snRNA; Prp24p; LSm2–8p proteins; RNA structure probing

*Corresponding author

Introduction

The precise excision of introns from pre-mRNAs involves two consecutive transesterification reactions that are catalysed by the spliceosome. This large and dynamic ribonucleoprotein complex is assembled on each intron in an ordered, multistep

process from the small nuclear RNPs (snRNPs) U1, U2, U4/U6 and U5, along with more than 100 non-snRNP proteins.^{1–3} Each of the snRNPs contains one RNA molecule and several proteins. Thus, the U4/U6 di-snRNP contains two RNAs, which are extensively base-paired.

During the assembly of the spliceosome and catalysis of splicing, the snRNPs undergo several precisely co-ordinated changes in composition and structure. This is particularly true of the U6 snRNP. The U6 snRNA base-pairs with the U4 snRNA to form, together with the respective proteins, the U4/U6 di-snRNP. The U6 snRNA undergoes major conformational changes during the formation of the U4/U6 di-snRNP. For example, nucleotides of the U6 snRNA that form an intermolecular stem-loop

Abbreviations used: snRNP, small nuclear RNP; RRM, RNA recognition motif; TAP, tandem affinity purification; DMS, dimethylsulfate; CMCT, 1-cyclohexyl-3-(2-morpholinoethyl) carbodiimide metho-*p*-toluene sulfonate; KE, β -ethoxy- α -ketobutyraldehyde; ISL, intramolecular stem-loop.

E-mail address of the corresponding author:
reinhard.luehrmann@mpi-bpc.mpg.de

(the 3' stem-loop), must be separated and positioned for base-pairing with the U4 RNA to yield stem II of the U4/U6 interaction domain.^{4,5} Similarly, the U6 nucleotides upstream of the 3' stem-loop base-pair with the U4 snRNA, forming stem I of the U4/U6 duplex in the di-snRNP. Thereafter, the U4/U6 di-snRNP associates with the U5 snRNP to form the U4/U6.U5 tri-snRNP, which enters the pre-spliceosome, containing the U1 and U2 snRNPs bound to the pre-mRNA. During the conversion of the fully assembled spliceosome into its catalytically active form, the base-pairing between the U4 and U6 snRNAs is disrupted and the U4 snRNP is released. Next, the U6 snRNA associates with the 5' splice site and base-pairs with the U2 snRNA, a step leading to the formation of the catalytically active centre.⁶⁻⁸ After splicing, the spliceosome dissociates and the released individual U4, U6 and U5 snRNPs are incorporated into new U4/U6 di-snRNPs and U4/U6.U5 tri-snRNPs in preparation for the next round of splicing.

The yeast U6 snRNP consists of the U6 snRNA, the specific protein Prp24p, and a set of seven Sm-like proteins (LSm2p, LSm3p, LSm4p, LSm5p, LSm6p, LSm7p, and LSm8p). The LSm2p-8p proteins form a seven-membered ring structure, very similar in appearance and size to that described for the Sm proteins of the snRNPs U1 to U5.⁹⁻¹¹ It has been shown that the LSm2p-8p complex binds to a uridine-rich sequence at the 3' end of U6 snRNA.^{9,12,13} In yeast, the LSm2p-8p proteins function as a chaperone complex that cooperates with Prp24p to support several rearrangements of U6-containing complexes.^{11,14} Prp24p, is an essential protein containing four RNA recognition motifs (RRMs) and is functionally related to the human splicing factor p110/SART3.^{15,16} Prp24p facilitates the formation of the U4/U6 di-snRNP from the individual U4 and U6 snRNPs in a process that does not require ATP, but which is more efficient in the presence of the LSm2p-8p proteins than with naked U6 snRNA.^{11,16-18} In this respect, it is interesting to note that Prp24p has been shown by yeast two-hybrid assays to bind specifically to all of the LSm2p-8p proteins except LSm3p.^{18,19} These interactions are consistent with the idea that Prp24p and the LSm complex cooperate in facilitating structural rearrangements. However, the exact mechanism of Prp24p function is not clear. One clue to the function of Prp24p could come from the information about its binding site on U6 snRNA and how Prp24p modulates the structure of the U6 snRNA in the U6 snRNP.

Chemical modification studies performed with U6 snRNPs enriched from yeast extracts by glycerol-gradient centrifugation, have indicated that Prp24p binds directly to nucleotides 40-43 of the U6 snRNA (see Figure 1).^{15,20} Recent *in vitro* binding experiments indicate that the primary binding site on the U6 snRNA of a C-terminally truncated form of Prp24p may lie within residues 45-58.²¹ However, the precise binding site of Prp24p on the U6 snRNA is not known. Several secondary structures of the yeast U6 snRNA,

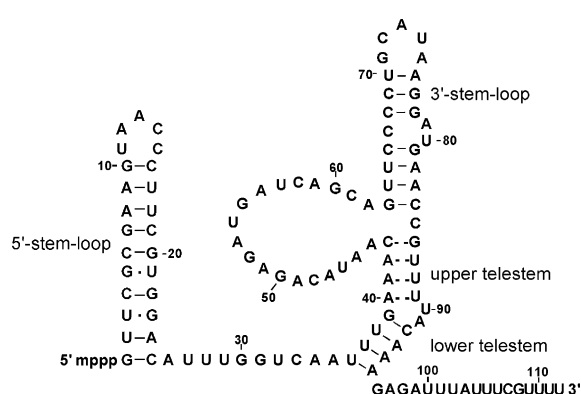


Figure 1. Proposed secondary structure model of the yeast *S. cerevisiae* U6 snRNA in the U6 snRNP.²² Nucleotides 36-39 and 92-95 define the lower telestem structure. Nucleotides 40-43 and 86-89 of the upper telestem structure are shown paired by open dashes, since their base-pairing interaction was not confirmed experimentally.²² Nucleotides 26-35, 44-62 and 96-112 are represented as undefined secondary structures.²²

based on genetic experiments and structure-probing of partially purified U6 snRNPs, have been suggested. However, the structure of the U6 snRNA in native U6 snRNPs is not clear.^{4,22,23} It was proposed that two distant regions of the U6 snRNA (positions 36-39, 40-43 and 86-89, 92-95, shown in Figure 1) have the potential to base-pair and form an intramolecular RNA duplex, called the telestem.^{23,24} It was suggested that the protection from chemical modifications of the U6 snRNA at bases 40-43 was due to base-pairing in the telestem and that the stem requires Prp24p only for its stabilisation.²³

As an initial step towards obtaining additional information about the binding site(s) of Prp24p on the U6 snRNA, as well as to shed light on the mechanism whereby Prp24p and the LSm complex facilitate U4/U6 base-pairing, we have investigated the secondary structure of the U6 snRNA in native, purified U6 snRNPs and compared it with its naked form.²⁵ We present here a detailed structural analysis of the native U6 snRNP using biochemical methods, including chemical structure probing, UV cross-linking and hydroxyl radical footprinting. The combined results demonstrate that the naked U6 snRNA structure is very compact, whereas in the presence of the Prp24p and the LSm2p-8p proteins, the RNA structure in the U6 particle is much more open. This is particularly apparent for the 3' stem-loop and a large internal asymmetrical loop of the U6 snRNA, in which several nucleotides are accessible in the U6 snRNP but are inaccessible to chemical modification in the naked U6 snRNA. We show that Prp24p binds strongly to the left part of the asymmetrical loop (nucleotides 40-60) and only moderately to the 3' stem-loop in the U6 snRNP. Our data suggest that Prp24p, in cooperation with LSm proteins, might be involved in opening these regions and thereby promote formation of stems I and II of the U4/U6 duplex. Interestingly, we find

that the structure of the yeast U6 snRNA in native snRNPs can be adopted by human U6 and U6atac snRNAs.

Results

Isolation of native U6 snRNPs from the yeast *Saccharomyces cerevisiae*, using the tandem affinity purification (TAP) method and C-terminally tagged Prp24p

To purify the yeast U6 snRNP for our structural investigations, we constructed a yeast strain containing TAP-tagged Prp24p and performed the TAP method.²⁵ The TAP tag consists of two IgG-binding domains of *Staphylococcus aureus* protein A and a calmodulin-binding peptide separated by a tobacco etch virus (TEV) protease cleavage site.²⁵ To obtain highly purified particles for mass spectrometric analysis,

a glycerol-gradient centrifugation step was included after TAP purification. Figure 2(a) shows the snRNAs distribution across the gradient. Fractions 15–18 contained U6 snRNA and was essentially free of all other snRNAs, as determined by silver staining of the gel (Figure 2(a)) and by Northern blotting (data not shown). In Figure 2(b), the protein composition of each fraction was analyzed by SDS-PAGE. Proteins co-sedimenting with the U6 snRNA in the peak fractions 16 and 17 were identified by mass spectrometry. Seven distinct proteins were found: Prp24p and six of the LSm2p–8p proteins, LSm4p, LSm7p, LSm8p, LSm2p, LSm5p, and LSm6p. This is essentially the same set of proteins that was found in purified U6 snRNPs,²⁶ with the exception of LSm3p, which probably eluded mass spectrometric detection. Indeed, the presence of LSm3p in our purified U6 snRNPs could be demonstrated independently by additionally tagging LSm3p (10 kDa) with

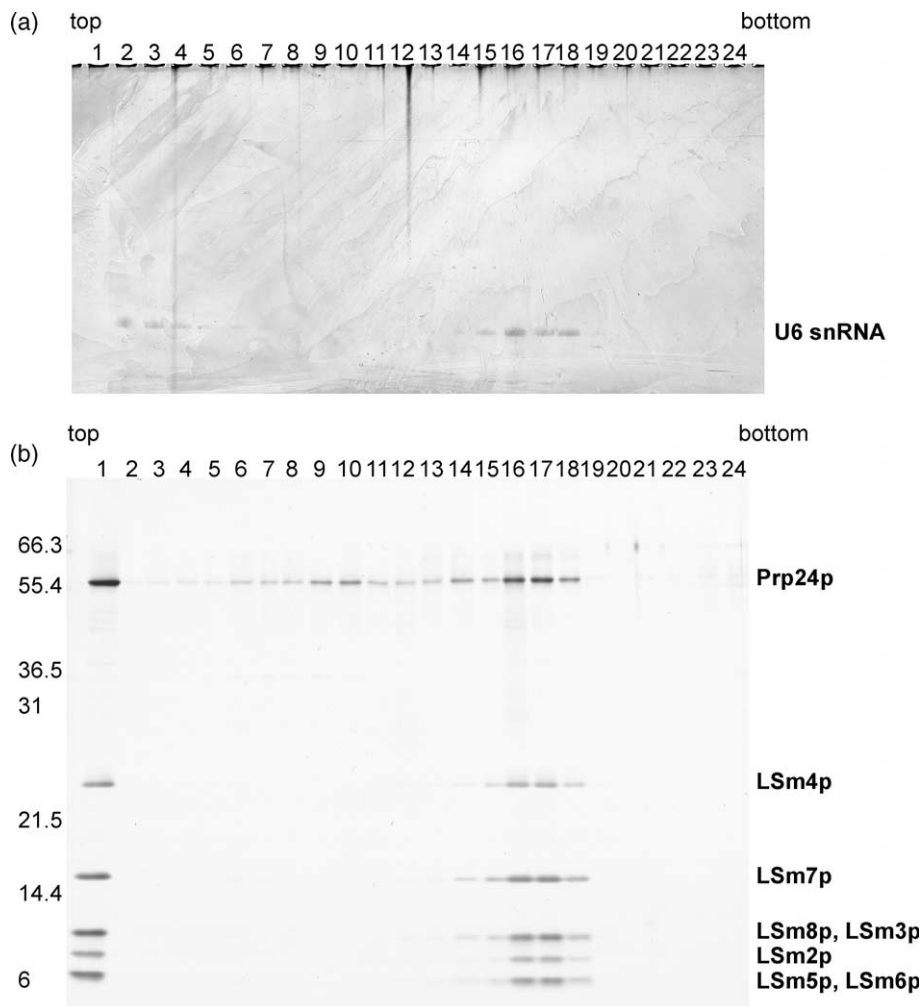


Figure 2. Characterization of the yeast U6 snRNP purified using the TAP method with tagged Prp24p. The U6 snRNP was purified from whole-cell extract by two affinity purification steps,²⁵ followed by centrifugation on a 10%–30% (v/v) glycerol gradient. Gradient fractions, numbered above each lane, were analysed for their (a) RNA and (b) protein content by denaturing PAGE or SDS-PAGE, respectively. Gels in (a) and (b) were stained with silver. The identity of the bands is indicated on the right.

a yECitrine 30 kDa tag²⁷ in the Prp24p-TAP tag strain. TAP tag purified U6 snRNPs contained stoichiometric amounts of Lsm3p-yECitrine fusion protein, which was detected as a 40 kDa protein (data not shown).

Determination of the secondary structure of naked U6 snRNA and U6 in purified U6 snRNP particles

The availability of highly pure U6 snRNPs allowed us first to investigate the structure of the U6 snRNA within these purified particles and, second, to determine how and where U6-associated proteins, in particular Prp24p, contact the RNA. We addressed these questions by initially analysing the structure of the RNA in the purified U6 snRNP and comparing it to that of the naked U6 snRNA obtained by *in vitro* transcription. For this purpose, we used three chemical reagents: dimethylsulfate (DMS), 1-cyclohexyl-3-(2-morpholinoethyl) carbodiimide metho-*p*-toluene sulfonate (CMCT) and β -ethoxy- α -ketobutyraldehyde (KE). These reagents act at the Watson-Crick base-pairing positions of a nucleotide: DMS modifies adenine and cytosine, CMCT modifies uracil and, to a lesser extent, guanine, while KE modifies guanine only.²⁸ Reactivity of a nucleotide towards any of these reagents is indicative of it being unpaired. Lack of reactivity indicates a paired status in the naked RNA and, either a paired status or an interaction with a protein in the RNP. Modifications were detected by primer extension with reverse transcriptase, which cannot read through the modified bases and stops after transcribing the nucleotide immediately preceding the modified base.²⁹

We used two oligodeoxynucleotides complementary to nucleotides 68–84 or 94–112, in order to analyse modifications of approximately 75% of all U6 snRNA nucleotides, ranging from nucleotides 2–89. Representative examples of the chemical probing experiments are shown in Figure 3. The modification patterns of naked U6 snRNA (lane 2 in each of Figure 3(a)–(f)) are compared directly to U6 snRNA in native U6 snRNPs (lane 3 in each of Figure 3(a)–(f)). The overall results, described in detail below, are summarised in Figure 3(g) and (h). Bases were assigned to a colour-coded group according to the intensity of modification observed. Blue implies no modification, pink implies only weak modification and red implies strong modification by the chemical reagent. The classification of bases in this manner, resulting from our analysis, is shown superimposed on the secondary-structure models of the naked U6 snRNA (Figure 3(g)) and that of the U6 snRNA in the snRNP particle (Figure 3(h)).

A first overall comparison of the naked U6 snRNA structure with that in the particle reveals that the RNA is very compact in the naked RNA state and more open in the protein-bound RNP state (compare Figure 3(g) and (h)). This is most pronounced in two regions. The first is the U6 3' stem-loop (nucleotides G63–C84). In the naked

RNA, most of the nucleotides are not modified, except for C72, which is highly modified. However, in the RNP, the very same structural element (i.e. nucleotides 63–84) contains six highly modified bases, with four out of five of the loop bases exposed to modifications (Figure 3(b) and (d), lanes 2 and 3).

The second region comprises nucleotides proposed to form the upper telestem (see Figure 1 and below for details). The three A nucleotides (A40–A42) assumed to form part of the ascending strand of the upper telestem are clearly accessible to modification by DMS in the naked RNA (Figure 3(a), lane 2). However, nucleotides U87–U89 (Figure 3(d), lane 2) proposed to form the descending strand of the upper telestem are not accessible to CMCT modification, suggesting that they are base-paired. Their most reasonable partners are G60, U57 and A56, which are also protected as shown in Figure 3(g) (blue disks). In conclusion, this demonstrates clearly that the upper telestem structure is not formed in the naked RNA.

Interestingly, nucleotides A40–A42 and U87–U89 show the opposite modification pattern in the U6 snRNP when compared to the naked RNA. Whereas adenosine bases A40–A42 are no longer accessible to modification (Figure 3(a), lane 3), nucleotides U87–U89 are fully accessible (Figure 3(d), lane 3). In fact, the whole region from C85 to U89 appears to be predominantly single-stranded (Figure 3(h)). We therefore conclude that the descending strand of the proposed upper telestem is essentially unpaired, making the existence of the upper telestem in the U6 snRNP also unlikely. Importantly, our footprinting data (see below) further indicate that protection of A40–A42 from modification in the U6 snRNP is most likely due to interaction with a protein. In contrast to the upper telestem, the lower telestem is compatible with our structure mapping data. In both the naked U6 snRNA and U6 snRNP, U36 to G39 were fully protected (Figure 3(c) and (e), lanes 2 and 3).

In addition, we reproducibly observed protection of G30–U32 in the U6 snRNA. The same nucleotides are somewhat less protected in the U6 snRNP (Figure 3(c) and (e), lanes 2 and 3). Their potential base-pairing partners are A99–U101. Although structural data for these latter nucleotides are difficult to obtain, we propose that this small helix (G30–C33, G98–U101) exists as an extension to the lower telestem in the naked U6 snRNA. However, the same helix may not be stable in the U6 snRNP. In conclusion, our data indicate that as a result of interaction of Prp24p and the LSm2p–8p proteins with U6 snRNA, a significant number of bases are more exposed in the snRNP than in the naked snRNA.

Mapping the binding region of the U6 proteins on the U6 snRNA by hydroxyl radical footprinting

As a next step in our characterisation of the protein/RNA interactions in purified U6 snRNP,

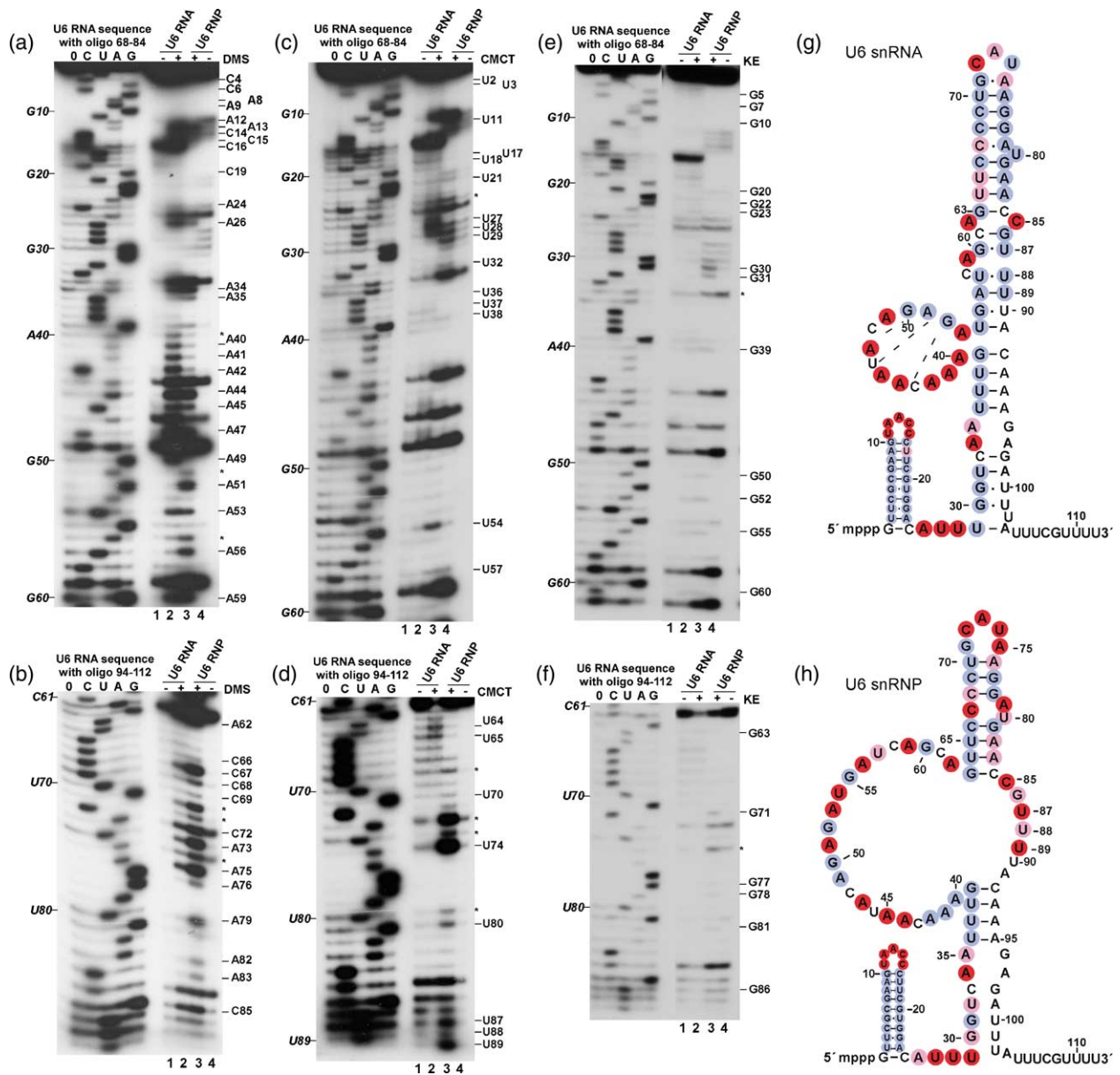


Figure 3. Structure-probing of purified U6 snRNPs with DMS, CMCT or KE. Primer extension reactions were carried out with two radiolabelled oligonucleotides, complementary to nucleotides 68–84 of the U6 snRNA ((a), (c) and (e)) or 94–112 ((b), (d) and (f)). In each gel, the positions where reverse transcription was blocked because of chemical modification of the base are shown on the right. Lanes C, U, A and G correspond to sequencing ladders made with the same oligonucleotide ("0", no ddNTP). Asterisks (*) indicate the nucleotides that showed an unusual reactivity to the chemical probes. Primer extension analyses of naked U6 snRNA (lanes 1 and 2 of each gel) and of U6 snRNA within isolated U6 snRNP (lanes 3 and 4) are shown. In each panel, in lanes 2 and 3 ("+" reagent) the reaction mixture was complete, while in lanes 1 and 4 ("–" reagent) the chemical reagent was omitted. (g) Comparison of the deduced secondary structures of naked U6 snRNA and (h) U6 snRNA in the snRNP. The accessibilities of the bases towards DMS, CMCT, and KE are represented by coloured disks superimposed on the secondary structure models of the naked (g) U6 snRNA and (h) of the U6 snRNA in the snRNP particle. Bases protected from modification, blue; bases weakly modified, pink; bases strongly modified, red.

we assayed protection of the RNA backbone in the particle by hydroxyl radical footprinting. Hydroxyl radicals attack the ribose moiety, leading to the excision of the base and scission of the ribose phosphate backbone.³⁰ Since susceptibility of the RNA backbone to hydroxyl radical cleavage is independent of secondary structure, protection of the ribose phosphate backbone from cleavage

results only from interaction with proteins or tertiary RNA–RNA interactions that mask the ribose moiety. The protection pattern of the U6 snRNA in the U6 snRNP from hydroxyl radical cleavage was analysed by primer extension as described above.

As shown in Figure 4(a), most of the nucleotides in the 5' half of the U6 RNA in the snRNP are protected

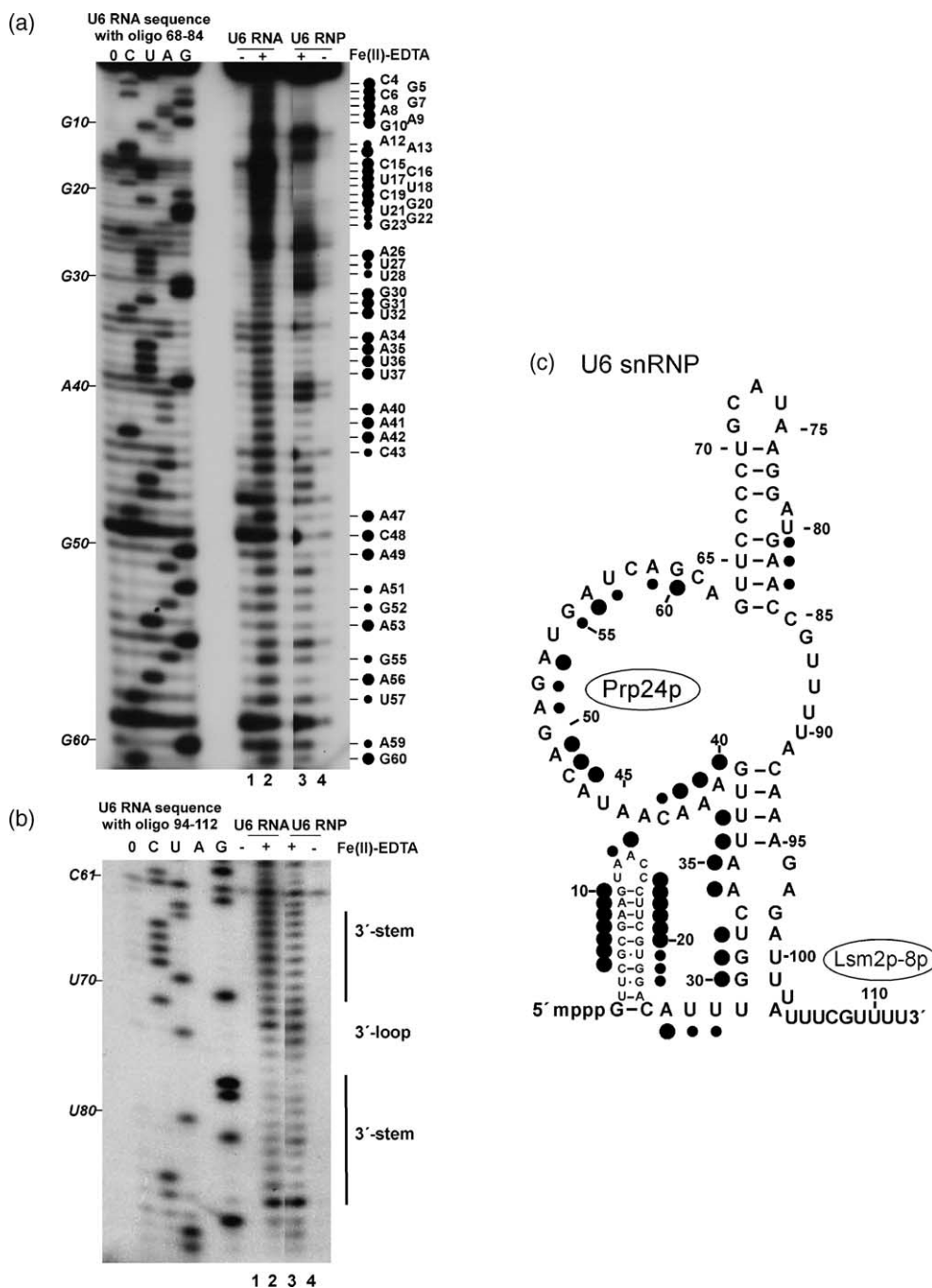


Figure 4. Mapping the binding regions of U6 proteins on the U6 RNA by hydroxyl radicals. Primer extension reactions were carried out with two radiolabelled oligonucleotides, annealed to the U6 snRNA at (a) nucleotides 68–84 or (b) 94–112. The nucleotide positions where reverse transcription was blocked due to the removal of the base are marked by black dots on the right. Lanes C, U, A and G correspond to sequencing ladders made with the same oligonucleotide. Note that in (b) the lane A is missing. Large dots indicate strong protection, and small dots indicate moderate or slight protection. Modification products from naked U6 snRNA (lanes 1 and 2 of each gel) and isolated U6 snRNP (lanes 3 and 4) are shown; in each case, for lanes 2 and 3 (“+” Fe(II)-EDTA) the reaction mixture was complete, while for lanes 1 and 4 (“–” Fe(II)-EDTA) hydroxyl radicals were omitted. (c) Summary of the U6 nucleotides protected from hydroxyl radicals in the U6 particle (black dots). The Figure shows the secondary structure of the yeast U6 snRNA in the U6 particle, which was established in this study.

to various degrees (see also Figure 4(c) for summary). A footprint is observed for nucleotides involved in base-pairing, as well as for single-stranded nucleotides, extending from C4 to G60. The 5' stem-loop appears to be complexed tightly with the protein(s):

nucleotides of both strands of the stem are protected, as well as two out of the five loop nucleotides. Also, several nucleotides of the large internal loop show various degrees of ribose protection, including A40, A41, A42 and C43 (Figure 4(a)). In contrast to the 5'

stem-loop, we find that the 3' stem-loop of the U6 snRNA in the U6 particle is not protected significantly from hydroxyl radical cleavage (Figure 4(b), compare lane 2 with lane 3). Only a few nucleotides may be protected slightly (i.e. positions 81, 82 and 83 of the descending 3' stem). Therefore, this region does not appear to be contacted strongly by U6 proteins.

Cross-linking of proteins to U6 snRNA: identification of Prp24p binding site(s)

To obtain independent evidence for contact points between proteins and the U6 snRNA, we performed

UV cross-linking of purified U6 particles. Affinity-purified U6 snRNPs were irradiated with UV light and then treated with proteinase K.³¹ The sites of cross-links were detected by primer extension: the peptide fragment attached to the RNA base blocks the progression of the reverse transcriptase on the RNA template, and the enzyme stops after transcribing the nucleotide immediately before the cross-linked base.³¹ As a control, identical experiments were carried out with naked U6 snRNA.

Figure 5(a) shows the primer extension analysis of the naked U6 snRNA (lanes 1 and 2) and U6 snRNA in the snRNP (lanes 3 and 4). The samples

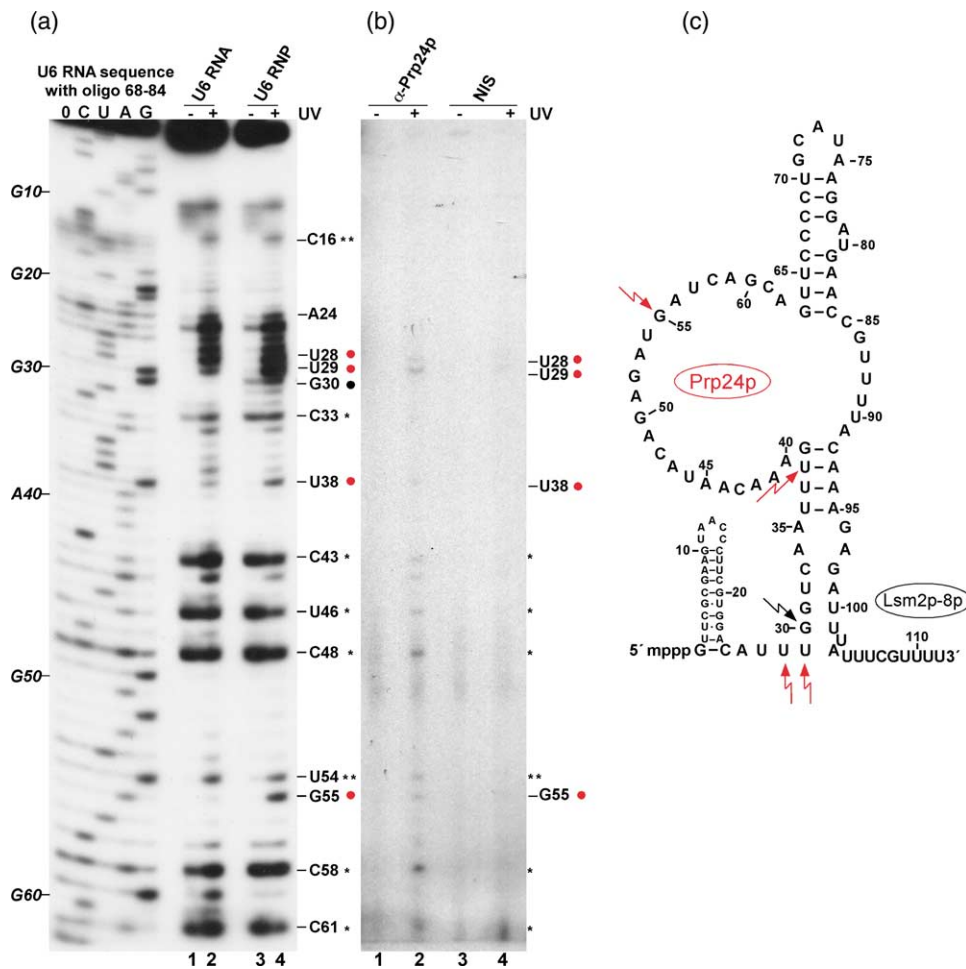


Figure 5. Prp24p can be cross-linked to U28, U29, U38 and G55 of the U6 snRNA in the U6 snRNP. (a) Primer extension analysis of UV-irradiated naked U6 snRNA (+UV, lane 2) and of U6 snRNA derived from UV-irradiated U6 snRNPs (+UV, lane 4). Lanes 1 and 3 are (control lanes with) primers extension analyses of non-irradiated naked U6 snRNA and U6 snRNA derived from non-irradiated U6 snRNPs (-UV). C, U, A and G are dideoxy sequence markers. Positions of nucleotides that caused a stop of reverse transcriptase are shown on the right. Note that the actual signals of reverse transcriptase stops are one nucleotide upstream of those that caused the block/stop (see the text for details). UV cross-linking sites of Prp24p on the RNA of the native U6 snRNP are marked by red dots and a putative UV cross-linking site of the Lsm2p-8p proteins at nucleotide G30 is marked by a black dot. The asterisks (*) indicate naturally occurring background stops (single asterisk) or putative RNA-RNA cross-links (double asterisks). (b) Primer extension analysis of the U6 snRNA after immunoprecipitation of denatured U6 snRNPs with an antibody raised against Prp24p (α -Prp24p),¹⁵ either with (lane 2) or without UV-irradiation (lane 1). The non-immune serum (NIS) was used as a control to precipitate UV-irradiated (lane 4) and non-irradiated (lane 3) particles. Nucleotide positions of reverse transcriptase stops due to specific cross-linking between Prp24p and the U6 snRNA are indicated on the right side with red dots. The asterisks indicate naturally occurring or UV-induced RNA-RNA background stops. (c) UV cross-linking sites of Prp24p on the RNA of the native U6 snRNP are marked by red arrows and a putative UV cross-linking site of the Lsm2p-8p proteins at nucleotide G30 is marked by a black arrow.

were UV-irradiated before (lane 4) or after (lane 2) isolation of the RNA from the U6 snRNP. Natural reverse transcriptase stops in the U6 snRNA occurred at nucleotides C33, C43, U46, C48, C58 and C61. These stops were detected irrespective of whether the samples had been UV-irradiated (Figure 5(a), compare lanes 1 and 3 with lanes 2 and 4). Prominent reverse transcriptase stops were observed at nucleotides C16, A24–U27 and U54 after UV-irradiation of both naked U6 snRNA and U6 snRNPs, suggesting that they do not represent protein–RNA cross-links but potentially RNA–RNA cross-links (Figure 5(a), compare lane 2 with lane 4). Additional UV-induced stops were detected at nucleotides G30, U38 and G55. These stops were found exclusively in the U6 snRNA isolated from UV-irradiated U6 snRNPs, indicating that they are caused by a cross-linked protein. However, it cannot be excluded that the presence of proteins in the U6 snRNP induces some new RNA–RNA cross-links by modulating the U6 snRNA structure. In addition, stops at U28 and U29 were enriched significantly in the U6 snRNP after UV irradiation, when compared with the UV-irradiated, naked U6 snRNA (Figure 5(a), compare lane 2 with lane 4). This suggests that they were also due to protein-specific cross-links to these nucleotides.

To determine which of these signals indeed corresponds specifically to Prp24p–U6 snRNA cross-links, UV cross-linked U6 snRNPs were disrupted with detergents (to dissociate all non-covalent interactions), immunoprecipitated with anti-Prp24p antibodies and then treated with proteinase K.³¹ Figure 5(b) shows the results of primer extension analyses of RNA species immunoprecipitated with anti-Prp24p antibodies before (lane 1) and after (lane 2) UV-irradiation. Reverse transcriptase stops were detected after immunoprecipitation at nucleotides U28, U29, U38 and G55 with the UV-irradiated particle only (Figure 5(b), lane 2). The remaining stops observed after UV-irradiation correspond to naturally occurring background stops or putative RNA–RNA cross-links (indicated by asterisks, compare Figure 5(a) with (b)). Controls show that RNA–protein cross-links were not immunoprecipitated with the non-immune serum either before (lane 3) or after (lane 4) UV-irradiation (Figure 5(b), lanes 3 and 4, NIS). In addition, a protein cross-linked to G30 was not immunoprecipitated by anti-Prp24p antibodies (compare lane 2 of Figure 5(b) with lane 4 of Figure 5(a)), indicating that G30 may be contacted by the LSM complex. We therefore conclude that Prp24p is cross-linked exclusively to U28, U29, U38 and G55 (summarized in Figure 5(c)).

Footprinting of recombinant Prp24p bound to the U6 snRNA

Hydroxyl radical footprinting performed with the native U6 snRNP suggested that Prp24p interacts within the first 60 nucleotides of the U6 snRNA. To investigate whether this region of the U6

snRNA is indeed bound only by Prp24p, and not by the LSM2p–8p proteins, we performed hydroxyl radical footprinting with *in vitro* transcribed U6 snRNA and recombinant Prp24p. U6 snRNA was incubated with increasing concentrations of recombinant Prp24p, and the resulting complexes were analyzed initially on a native polyacrylamide gel (Figure 6(a)). Recombinant Prp24p shifted the U6 snRNA quantitatively to a slower migrating complex at the highest concentrations tested and only one RNP complex was observed (Figure 6(a), lane 4 and 5). We thus conclude that the binary U6 snRNA–Prp24p complex is homogeneous.

Analysis of the U6 snRNA–Prp24p complexes by hydroxyl radical footprinting revealed a U6 snRNA protection pattern similar to that seen with the native U6 snRNP (Figure 6(b), middle panel, black bars). The 5' stem–loop structure could not be discerned well in these experiments. Therefore, we analyzed this region more closely using an oligonucleotide complementary to nucleotides 68–84 of U6 snRNA (Figure 6(b), left panel). The 5' stem–loop appears to be protected, but not as strongly as in the native particle. Nucleotides A26–G60 of the U6 snRNA were protected strongly (with a few exceptions), demonstrating that recombinant Prp24p binds the U6 snRNA in the C4–G60 region. Interestingly, the protection pattern of the large loop region is very similar to that of the same region in the native particle, excluding only a few nucleotides, such as, for example, A45, G50 and U54, which seem protected more strongly by recombinant Prp24p. We thus conclude that the large internal loop binds exclusively Prp24p also in the native U6 particle.

Unexpectedly, although the 3' stem–loop was not protected by proteins in the native U6 snRNP, a protection of the 3' stem, comprising nucleotides A62–G71, A75–A79 and G81–A83, was observed with the binary complex (Figure 6(b), grey bars). In agreement with previous experiments performed with recombinant Prp24p,^{21,32} this indicates that recombinant Prp24p interacts also with the 3' stem when the LSM proteins are missing (see Figure 6(c) for a summary; dots indicate the protection pattern obtained). This may suggest that either Prp24p expressed in *Escherichia coli* behaves differently than native Prp24p or that the presence of the LSM complex in the native U6 particles modulates the specificity of Prp24p binding.

Discussion

The secondary structure of U6 snRNA in purified U6 snRNPs differs significantly from that of naked U6 snRNA

Our chemical modification data demonstrate that the naked U6 snRNA structure is dramatically different from the structure of the U6 snRNA in U6 snRNP particles (Figure 7(a)). The structure of the naked U6 snRNA is very compact, whereas the

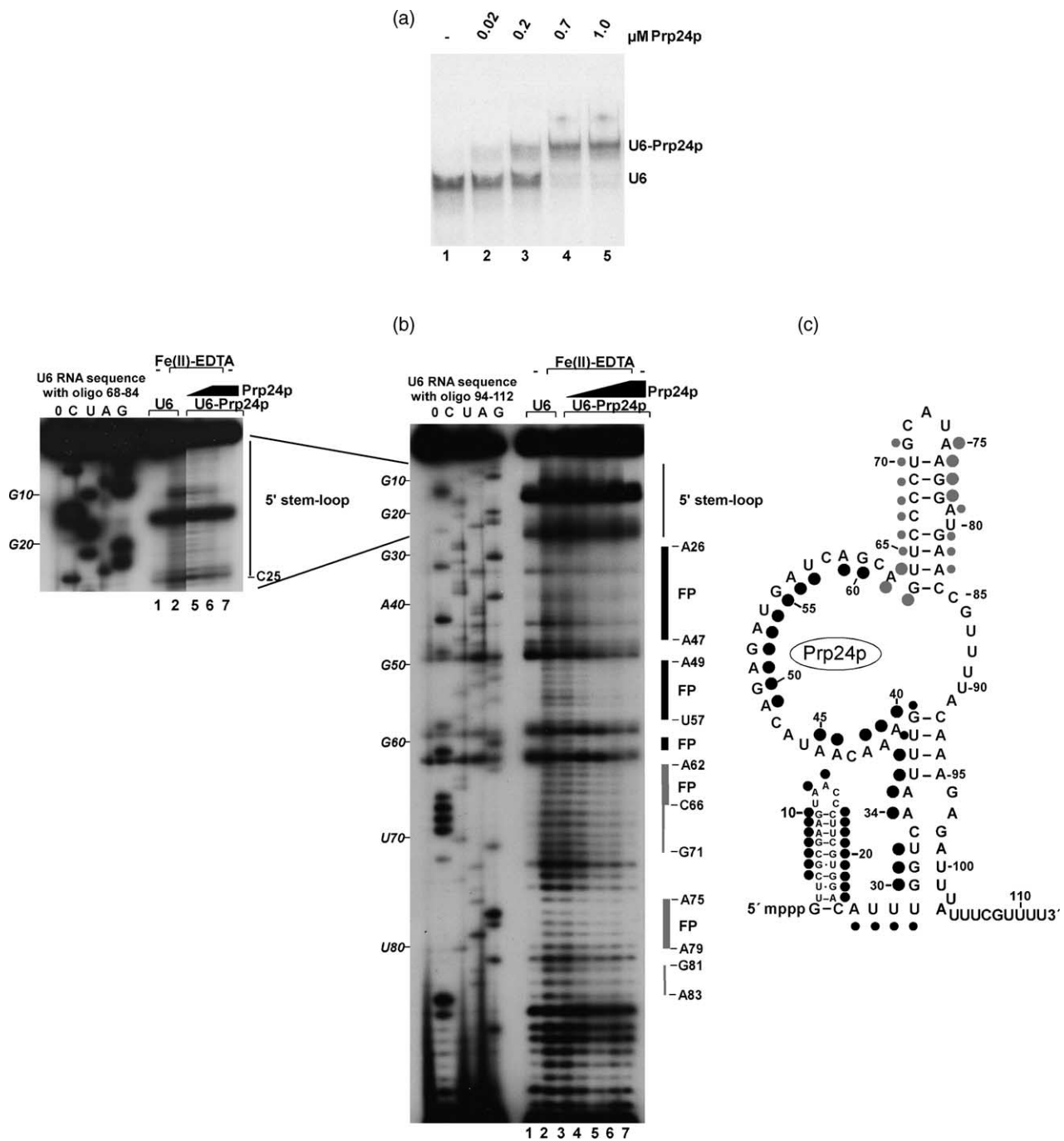


Figure 6. Analysis of complexes formed between recombinant Prp24p and *in vitro* transcribed U6 snRNA. (a) A sample (0.6 pmol) of ^{32}P -labelled U6 snRNA was incubated in the absence (lane 1), or in the presence of increasing concentrations of recombinant Prp24p (lane 2, 0.02 μM; lane 3, 0.2 μM; lane 4, 0.7 μM; lane 5, 1 μM), and complexes were then analysed on a native polyacrylamide gel. (b) Hydroxyl radical footprinting of the U6 snRNA-Prp24p complex. The Fenton reagent-treated complexes were analysed by primer extension using a radiolabelled oligonucleotide complementary to the U6 snRNA at positions 94–112 (middle panel) and 68–84 (left panel). The protection of the ribose backbone from hydroxyl radicals at increasing concentrations of recombinant Prp24p (lanes 3–6, 0.02 μM, 0.2 μM, 0.7 μM and 1 μM), is marked by black bars on the right side of the Figure and designated as FP (footprint). Grey bars indicate mild protection. Lanes 1 and 2 contain the U6 snRNA as described in Figure 4. Lane 7 consists of untreated U6 snRNA-Prp24p complexes, which were obtained by incubating the U6 snRNA with recombinant Prp24p at a concentration of 1 μM. (c) Summary of the U6 snRNA protection from hydroxyl radicals due to recombinant Prp24p (black and grey dots). The Figure shows the secondary structure of the yeast U6 snRNA in the U6 particle, which was obtained by this study.

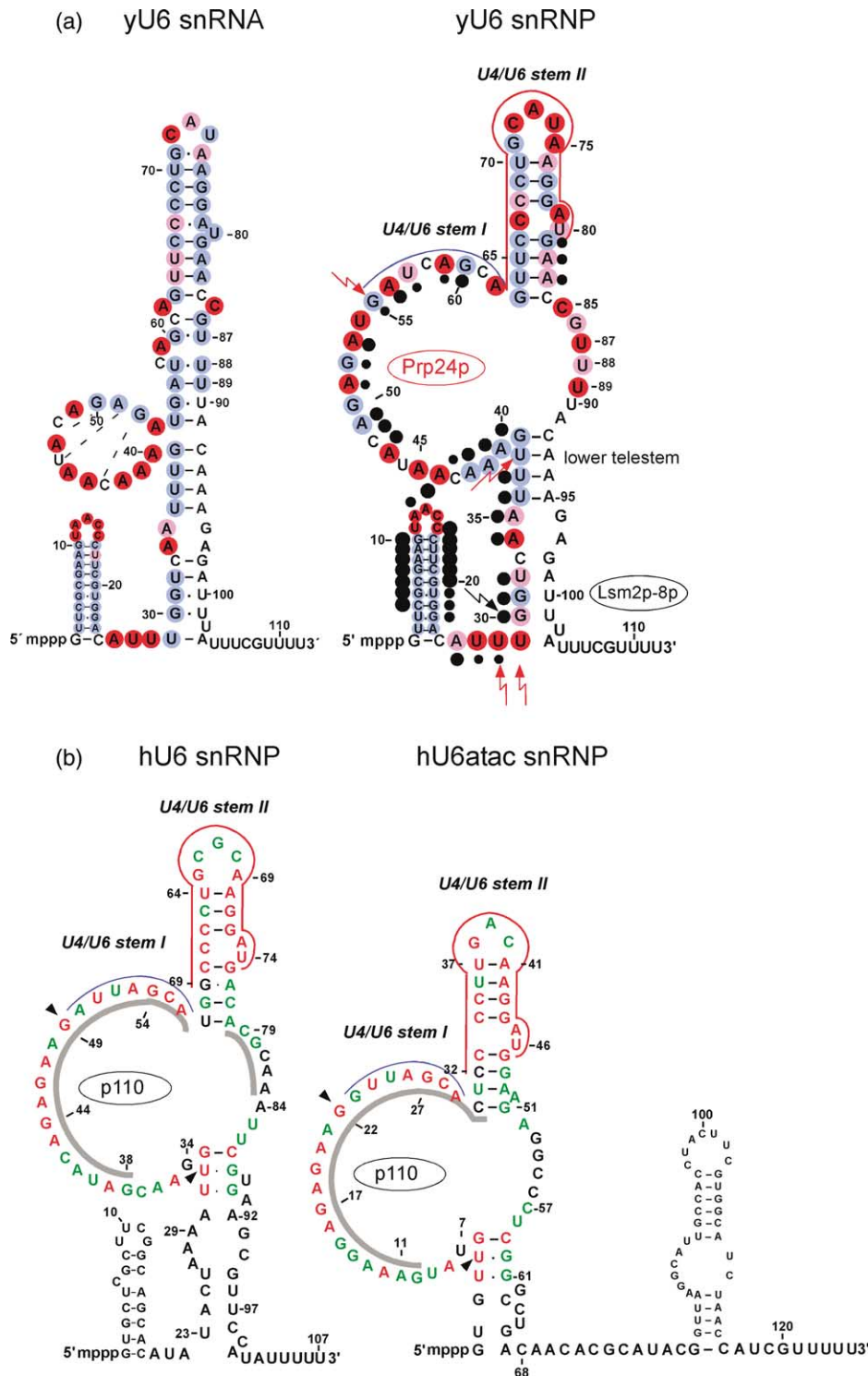


Figure 7. (a) Comparison of the proposed secondary structure of yeast U6 snRNA in the naked and in native U6 snRNPs obtained by chemical structure probing. The binding region of Prp24p on the U6 snRNA was determined by hydroxyl-radical footprinting (black dots) and UV cross-linking (red arrows); for details, see the text. (b) The structures of the U6 and U6atac snRNAs in the human and human U6atac particles, respectively, have been extrapolated from the structure of the yeast U6 snRNA with the U6 snRNP shown in (a); see the text for details. The recognition element of the human orthologue of Prp24p, p110/SART3, is depicted in grey.^{16,43} The black arrowheads point to two of the evolutionarily conserved nucleotides that in yeast are UV-crosslinked to Prp24p. Nucleotides that are 100% evolutionarily conserved between yeast U6, tomato U6, nematode U6, fly U6, mouse U6, human U6 and human U6atac snRNAs are shown in red. Nucleotides that are 70% conserved are shown in green. In each part of the Figure, nucleotides that are involved in the formation of stems I and II with the U4 snRNA, are highlighted with blue and red lines, respectively.

presence of Prp24p and the LSm2p–8p proteins leads to a more open snRNA structure in the U6 particle. This is particularly apparent for the 3' stem–loop (or intramolecular stem–loop, ISL, nucleotides 63–84), in which several nucleotides are inaccessible to chemical modification in the naked U6 snRNA, but are accessible in the U6 snRNP (Figure 7(a)). Our data for the naked RNA are consistent with the NMR structure of a portion of the U6 ISL. For example, the proposed A79·C67 wobble pair³³ is consistent with the total (A79) and partial (C67) protection from chemical modification that we observe. Similarly, the complete protection of U80 under our conditions, is consistent with NMR studies performed at pH 7.0 that showed that U80 is sequestered within the helix.³³ In the U6 snRNP, we observe a significant increase in the reactivity of bases C67 and A79 and, to a certain extent, of U80. Remarkably, we observe that the reactivity of bases C72–A75 of the loop structure is also enhanced when compared with that of the naked RNA.

In addition, our chemical modification data show that several nucleotides below the 3' stem–loop (e.g. 54–62 and 87–89) are paired in the naked U6 snRNA. A notable exception is the small internal loop, in which only three of the nucleotides are inaccessible; the latter could potentially form intramolecular base-pairings, as shown in Figure 7(a) (broken lines). In this region, there is a dramatic difference between the structure of the naked U6 snRNA and the U6 snRNA in the U6 particle. The presence of the U6 proteins leads to restructuring of these nucleotides, as can be seen especially for nucleotides 54–62 and 87–89, which are single-stranded only in the U6 snRNP. Remarkably, the presence of Prp24p and the LSm complex leads to a number of local structural rearrangements, resulting in an opening of the U6 snRNA structure. Dissociation of base-pairing results in the formation of the large asymmetric internal loop, which is composed of a left loop (A40–A62) and a right loop (C85–A91). This has important functional implications, as discussed below.

The same holds true for the stem at the base of the U6 snRNA, where nucleotides 29–33 can base-pair with nucleotides 96–103 in the naked RNA. The RNA within the U6 particle seems to be less compact also in this region. Indeed, nucleotides in the 28–54 region were previously found to be available for oligonucleotide-directed RNase H cleavage in the yeast U6 snRNP in cell extracts.³⁴ This also may be due to the fact that several nucleotides of the large internal loop are single-stranded and available for base-pairing with an oligonucleotide. This would again indicate that the presence of proteins loosens the U6 snRNA structure (Figure 6(a)).

Our data do not support the presence of the upper half of the previously proposed telestem. We show that bases A40–A42 are single-stranded in the naked U6 snRNA, whereas they are protected from modifications in the U6 snRNP, indicating that these

bases are either paired or shielded by Prp24p. However, we demonstrate clearly that bases A40–A42 are not paired, since their proposed binding partners, U87–U89, are accessible to the chemical probing reagents (Figure 7(a)). This is consistent with data reported by Ryan *et al.*, who proposed that this half of the telestem, which would form between bases A40–C43 and G86–U89, binds Prp24p even when the Watson–Crick base-pairing is disrupted by mutation of nucleotides G87–U89.²² Moreover, Ghetti *et al.* observed that mutation of bases A40 and C43 decreased binding of recombinant Prp24p to naked U6 snRNA,³² suggesting that Prp24p contacts these bases in a sequence-specific manner.²² In addition, our footprinting analysis shows that nucleotides A40–C43 are protected from hydroxyl radical cleavage in native U6 snRNPs. Thus, this demonstrates that bases A40, A41, A42 and C43 are unpaired, but protected by direct binding of Prp24p, as discussed below.

In agreement with previously proposed yeast U6 secondary structures, we demonstrate that bases U36–G39 of the lower half of the telestem are paired in both the naked U6 snRNA and the RNA of the U6 particle (Figure 7(a)). Bases A26–U28 are accessible to modification reagents, both in the naked U6 snRNA and in the U6 snRNP particle, suggesting that they are unpaired.³⁵

The binding site of Prp24p on the U6 RNA in the U6 snRNP particles

Our hydroxyl radical footprinting experiments revealed that U6 proteins protect most of the nucleotides in the region C4–G60 of the U6 snRNA in native U6 snRNPs (see the black dots in Figure 7(a)). A similar region was protected when footprinting was performed with a binary recombinant Prp24p–U6 snRNA complex. The combined results of these footprinting studies indicate that the 5' half of the U6 snRNA is the major binding region of Prp24p. Consistent with our footprinting data, we show by UV cross-linking that Prp24p contacts the U6 snRNA directly at four positions within the C4–G60 region (see the red arrows in Figure 7(a)). The left part of the large asymmetrical loop (A40–A62) is the most attractive binding site of Prp24p. Two types of Prp24p protections are found in this region: (i) bases protected at the Watson–Crick positions and on the ribose moiety; and (ii) bases freely accessible at the Watson–Crick positions but protected on the ribose moieties. A40–C43, A49, G52, G55 and G60, whose bases must form intimate contacts with Prp24p belong to the first type of protection (Figure 7(a), blue). It is interesting to note that A40–A42 are among the few nucleotides; freely available in the naked U6 snRNA and could represent a recognition motif for nucleation of Prp24p. A47, A51, A53, A56 and A59 belong to the second type (Figure 7(a), red). Interestingly, two of them are in the upper portion of the large loop (i.e. G55–A60), which is the region of U6 snRNA

involved in base-pairing with U4 snRNA to form the stem I duplex.

Using recombinant Prp24p, we observe that the footprint on the U6 snRNA extends to the entire 3' stem. One possibility to explain this broader binding region is that Prp24p expressed in *E. coli* binds less accurately than native Prp24p. Another possibility might be that Prp24p binds correctly to the U6 snRNA only when the LSm proteins are present. This is observed also, in part, for the 5' stem-loop structure. A protection of the 5' stem-loop is clearly seen after hydroxyl radical footprinting of the U6 snRNP. A similar protection is visible in the *in vitro* reconstituted U6-Prp24p binary complex; however, recombinant Prp24p binds the 5' stem-loop less efficiently. Again, this could, in part, be due to recombinant Prp24p itself. However, we favour the hypothesis that the LSm complex helps Prp24p to bind the 5' stem-loop more tightly and, overall, to bind the U6 snRNA more specifically.

Prp24p and the LSm complex facilitate U4/U6 association by opening the U6 structure

Our results demonstrate that a large asymmetric internal loop region of the U6 snRNA in the U6 particle is unpaired and protected from chemical modification by bound Prp24p. Prp24p interacts alternatively with bases or ribose moieties in this region, and thus several of the bases whose sugar backbone is contacted by Prp24p are available for base-pairing interaction. This complex interaction of Prp24p with the large asymmetric loop of the U6 snRNA should facilitate pairing of the G55–A62 bases of the U6 snRNA with the complementary U4 snRNA bases to form the U4/U6 stem I duplex.

In addition, a similar protein-induced exposure of specific nucleotides is seen in the 3' stem-loop. We show that the 3' stem-loop is not bound tightly by U6 proteins in native particles. However, in the presence of Prp24p and the LSm2p–8p proteins, the 3' stem-loop assumes a more open conformation. This is in agreement with the results of previous genetic experiments. That is, point mutations in the U6 snRNA that hyperstabilise the 3' stem-loop in the cold could be suppressed by mutations in the RRM2 and RRM3 of Prp24p.^{4,23} These experiments indicate that Prp24p might indeed be involved, together with the LSm complex, in opening the 3' stem to allow formation of stem II (U64–U80 in U6) in the U4/U6 duplex.^{4,23}

It is interesting to note that the 3' stem-loop resembles a so-called kissing loop.³⁶ U6 and U4 intermolecular base-pairing may begin between the unstructured free 5' end of the U4 snRNA and the complementary 3' stem-loop of the U6 snRNA, leading to helix propagation to form stem II in the U4/U6 di-snRNP. Helix propagation would indeed be greatly facilitated in the snRNP, since the presence of Prp24p and the LSm2p–8p proteins, as shown above, destabilizes the stem. U80 and A79 of the bulge, as well as C72, A73 and U74 of the loop,

are unpaired and therefore readily available for interaction with their binding partners in the U4 snRNA. Such initial recognition of the U4 snRNA by the 3' stem-loop of the U6 snRNA may lead to destabilization of surrounding RNA structures located on either side of the binding site, thereby allowing new RNA/RNA interactions to form. After formation of stem II, Prp24p may “hand over” to the U4 snRNA the single-stranded binding region G55–A62 for the formation of stem I.

In conclusion, our data suggest that the combined association of Prp24p and the LSm complex confers upon U6 nucleotides a conformation favourable for U4/U6 base-pairing. Thus, Prp24p and the LSm proteins may act as RNA chaperones.^{11,21} It has been hypothesized that RNA chaperones and specific RNA-binding proteins can solve different problems in RNA folding.^{37,38} A role as RNA chaperones for the LSm proteins was proposed previously.¹⁴ The LSm complex would help facilitate U6 snRNA restructuring, and the specific RNA-binding protein Prp24p would stabilize the active U6 snRNA structure, which would not be sufficiently stable on its own.³⁷ Indeed, recombinant Prp24p in the absence of the LSm proteins binds to the entire 3' stem of U6 snRNA. This binding would probably block or slow the opening of this sequence, which is required to form the stem II duplex with the U4 snRNA.

The structure of the yeast U6 snRNA in native snRNPs can be adopted by human U6 and U6atac snRNAs

In contrast to the other yeast spliceosomal RNAs, U6 is very similar in size and sequence to its human counterpart. Therefore, U6 snRNA from yeast and man may be expected to assume similar secondary structures. In fact, these molecules have a 3' stem-loop of similar length (see Figure 7(a) and (b)).^{4,39,40} The same holds true for the U6atac snRNA, the 3' stem-loop of which has been shown to be phylogenetically conserved (Figure 7(b)).⁴¹ Up to now, human U6 mono-snRNPs have not been isolated, however, the structure of naked U6 snRNA of higher eukaryotes was obtained by theoretical calculations of maximal base-pairing and by chemical and enzymatic probing.^{35,39} In both cases, the structure of the human U6 snRNA is very compact and resembles very much the structure of our naked yeast U6 snRNA. The existence of an internal loop was predicted,⁴² and it may be analogous to the loop adopted by bases 40–53 of the yeast U6 snRNA (Figure 7(a)).

It was shown recently that the mammalian counterpart of Prp24p, p110/SART3, binds an internal region of the human U6 snRNA (bases 38–57) and a 5' stem-loop of the U6atac snRNA from the same species (bases 10–30).^{16,43} These nucleotides exhibit a high level of evolutionary conservation between these two functionally related snRNAs, so it would be unexpected if they were to differ significantly in their secondary

structure.⁴³ To determine whether the human U6 and U6atac snRNAs fold according to the yeast secondary structure obtained from our studies, we have aligned the yeast, human and U6atac snRNA sequences (data not shown). Taking into consideration evolutionarily conserved nucleotides, the binding region of Prp24p to the yeast U6 snRNA in the native particle, and the binding region of recombinant p110 to the human U6 and U6atac snRNAs,⁴³ we propose the structures that are shown in Figure 7(b). These structures suggest that the binding of both Prp24p and its mammalian orthologue p110 to the U6 snRNA would occur mostly at an internal loop of RNA consisting of several highly evolutionarily conserved bases.²¹ In addition, the presence of similar recognition elements, conserved during evolution, implies that the structures of the U6 snRNAs in these particles, and the function of a protein capable of promoting functionally active RNA conformations (such as Prp24p/p110), is related among organisms.

Figure 7(b) shows also that two of the nucleotides (U38 and G55), which are cross-linked to Prp24p, are 100% conserved in evolution, and that G55 is situated in a highly conserved region of the yeast U6 snRNA found also in the human, as well as in the human and fly U6atac snRNA. This suggests that conservation of these nucleotides in U6 snRNA may be related to their role in Prp24p/p110 binding and in spliceosomal function, such as base-pairing with the U4 and subsequently with the U2 snRNAs.

Materials and Methods

Strains and plasmids

To construct the yeast strain expressing TAP-tagged Prp24p, the C-terminal TAP cassette was amplified by PCR from the plasmid pBS1479.²⁵ This PCR product was used to transform haploid yeast cells and transformants were selected on SD drop-out medium lacking tryptophan.²⁵ The resulting strain, YRK3 (MATa *trp1*- Δ 1, *his3*- Δ , *ura3*-52, *lys2*-801, *ade2*-101, *PRP24*::TAP-tag *K.I.TRP1* C terminus) carries a single chromosomal copy of the *PRP24* gene, containing the TAP tag and the *K.I.TRP1* marker at its C terminus. The construction of the yeast strain expressing the yECitrine-tagged LSm3p cassette²⁷ will be published elsewhere.

Purification of U6 snRNP and mass-spectrometric identification of its proteins

Purification of snRNPs was performed as described.²⁵ Briefly, yeast cells were grown in 2 l of YPD medium to an A_{600} of 2.5 and were disrupted by passing once through a French press at a pressure of 150 MPa (21,800 psi). The U6 snRNP was isolated from the cell extract by two purification steps, employing first an IgG matrix and then calmodulin-coated beads.²⁵ For analysis by mass spectrometry, the U6 snRNP isolated from 6 l of culture was further subjected to centrifugation in a 10%–30% glycerol gradient, run at 45,000 rpm for 15 h at 4 °C using a Sorvall TH-660 rotor.⁴⁴ Proteins from the gradient fractions were separated on a high-*N,N,N',N'*-tetramethylethylenediamine (TEMED),

SDS/12% (w/v) polyacrylamide gel and stained with silver. The visible protein bands of fraction 16, containing the greatest amount of U6 snRNP (Figure 2) were cut out and digested with trypsin by the method of Shevchenko.⁴⁵ When a protein could not be identified unambiguously by matrix-assisted laser desorption/ionization mass spectrometry, liquid chromatography tandem mass spectrometry was performed.⁴⁵

Prp24p overexpression and purification

The *PRP24* gene was amplified by PCR from yeast genomic DNA. The resulting fragment was double-digested with NcoI/Acc65I and subcloned into an NcoI/Acc65I-digested pETM-11 plasmid containing a His₆ tag. The resulting plasmid was introduced in the *E. coli* strain Rosetta (DE3, pLYSs). A 1 culture of the Rosetta cells was grown at 37 °C in growth medium containing 30 mg/l of kanamycin and 30 mg/l of chloramphenicol until the cells had reached an A_{600} of 0.3. IPTG was then added to a final concentration of 2 mM and incubation was continued overnight at 25 °C. The cells were harvested and shock-frozen in liquid nitrogen. The cell pellet was resuspended in ice-cold lysis buffer (20 mM Tris-HCl (pH 8.0), 150 mM NaCl, 10 mM imidazole, 0.2% (v/v) NP-40, 2 mM β -mercaptoethanol, 10 mg of lysozyme, and EDTA-free protease inhibitors (Roche) and incubated for a further 10 min on ice). The cells were disrupted by sonication while cooling with ice-cold water. A cleared lysate was obtained by centrifugation at 11,200 rpm for 30 min at 4 °C, using a Sorvall SS34 rotor. Nucleic acids were removed from the cleared lysate by precipitation with 3% (w/v) streptomycin sulfate (CalBioChem), followed by centrifugation as above. The supernatant containing Prp24p was loaded onto a Polyrep column (BioRad) containing 1 ml of Ni-NTA agarose beads (Qiagen) and incubated for 1 h at 4 °C. His-tagged Prp24p was eluted with 325 mM imidazole.

Chemical modification, UV cross-linking and footprinting experiments

The modification reagents used were dimethylsulfate (DMS; FLUKA, Buchs, Switzerland), 1-cyclohexyl-3-(2-morpholinoethyl) carbodiimide metho-*p*-toluene sulfonate (CMCT; Sigma, St Louis, MO, USA) and β -ethoxy- α -ketobutyraldehyde (KE; Research Organics, Cleveland, OH). For the modification reactions, 3.3 pmol of native U6 snRNP or of U6 snRNA prepared by transcription *in vitro*³⁴ were incubated with modification reagents in the presence of 1 μ g of *E. coli* tRNA, essentially as described.²⁹ To recover the RNA, the sample was first precipitated by adding three volumes of ethanol in the presence of 10 μ g of glycogen (Ambion), extracted with phenol/chloroform/isoamyl alcohol (PCI: 25:24:1 by vol.) in the presence of 0.1% (w/v) SDS, and precipitated by adding ethanol. After washing with 1 ml of 70% ethanol, samples were dissolved in 3.5 μ l of CE buffer (10 mM cacodylic acid/KOH (pH 7.0), 0.2 mM EDTA). Then 1 μ l of modified RNA was analysed by primer extension using [³²P]oligonucleotides. The primer extension analysis was performed as described.⁴⁶ Modification with DMS was carried out in 200 μ l of CKM buffer (50 mM cacodylic acid/KOH (pH 7.0), 50 mM KCl, 10 mM MgCl₂), as described.⁴⁶ The reaction was allowed to proceed in the presence of 2.5 μ l DMS on ice for 40 min, and then stopped by the addition of 50 μ l of DMS stop buffer (1 M Tris-HOAc (pH 7.5), 2 M β -mercaptoethanol, 12.5 mM EDTA); the RNA was then recovered as described above. CMCT

modifications were performed in 100 μ l of borate buffer (50 mM borate/KOH (pH 8.0), 50 mM KCl, 10 mM MgCl₂, 12.5 μ l of 0.4 M CMCT) and samples were incubated on ice for 60 min. The reaction was stopped by precipitation with ethanol. KE modifications were carried out in 100 μ l of KE buffer (50 mM cacodylic acid/KOH (pH 7.0), 50 mM KCl, 10 mM MgCl₂). After addition of 2 μ l of KE buffer, the reaction was allowed to proceed for 80 min on ice, stopped by adding KE stop buffer (3 M sodium acetate (pH 5.2), 50 mM borate/KOH (pH 7.0)) and precipitated by adding ethanol. The pellet was then resuspended in TES/borate buffer (10 mM Tris-HCl (pH 7.5), 50 mM borate/KOH (pH 7.0), 1 mM EDTA, 0.1% (w/v) SDS), extracted with PCI and precipitated by adding ethanol. Finally, the RNA was dissolved in 3.5 μ l of CE/borate buffer (10 mM cacodylic acid/KOH (pH 7.0), 0.2 mM EDTA, 50 mM borate/KOH (pH 7.0)). For UV-cross-linking studies, affinity-purified U6 snRNPs were irradiated for 2 min with UV light at 254 nm and immunoprecipitated under denaturing conditions as described:³¹ 3.5 pmol of native U6 snRNP or native U6 snRNA, which was isolated from native U6 snRNPs by digestion with proteinase K followed by extraction with PCI, was used. Cross-linking products were analysed by primer extension as described above.

For hydroxyl radical footprinting experiments with native U6 snRNP, 3.3 pmol of isolated particles were diluted to 200 μ l with DMS buffer and then incubated after addition of 1 μ g of *E. coli* tRNA, with 8 mM Fe(II)-EDTA in the presence of 0.005% (v/v) H₂O₂ and 5 mM ascorbic acid to initiate hydroxyl radical formation. Naked U6 snRNA, prepared by transcription *in vitro*, was incubated with 0.5 mM Fe(II)-EDTA in the presence of 1 μ g of *E. coli* tRNA, 0.005% H₂O₂ and 5 mM ascorbic acid as described above. For hydroxyl radical probing of the U6-Prp24p complexes, 0.6 pmol of U6 snRNA prepared by transcription *in vitro* was incubated for 1 h at 4 °C with increasing amounts of recombinant Prp24p (0.02 μ M, 0.2 μ M, 0.7 μ M, and 1 μ M) in a final volume of 40 μ l of binding buffer (30 mM Tris-HCl (pH 7.5), 150 mM NaCl, 8 mM MgCl₂, 2 mM DTT, 0.4 μ g of *E. coli* tRNA (10 μ g/ μ l), 1.6 μ g of BSA (40 μ g/ μ l), 0.1% (v/v) Triton X-100). Subsequently, the reaction mixture was diluted with CKM buffer (see above) to a final volume of 200 μ l and the reaction was initiated with 0.5 mM Fe(II)-EDTA, 0.003% H₂O₂, and 2.5 mM ascorbic acid. The cleavage products were identified by primer extension as described above.

Acknowledgements

We are very grateful to Cindy Will for critical comments. We thank Marion Killian and Monika Raabe for technical assistance. We thank Christine Guthrie for the gift of anti-Prp24p antibodies. This work was supported by grant DFG LU294/12-1 to R. L.

References

- Will, C. L. & Lührmann, R. (2001). Spliceosomal UsnRNP biogenesis, structure and function. *Curr. Opin. Cell. Biol.* **13**, 290–301.
- Burge, C. B., Tuschl, T. & Sharp, P. A. (1999). Splicing of precursors to mRNAs by the spliceosomes. In *The RNA World II* (Gesteland, R. F., Cech, T. R. & Atkins, J. F., eds), pp. 525–560, Cold Spring Harbor Laboratory Press, Cold Spring Harbor, NY.
- Jurica, M. S. & Moore, M. J. (2003). Pre-mRNA splicing. awash in a sea of proteins. *Mol. Cell.* **12**, 5–14.
- Fortner, D. M., Troy, R. G. & Brow, D. A. (1994). A stem/loop in U6 RNA defines a conformational switch required for pre-mRNA splicing. *Genes Dev.* **8**, 221–233.
- Wolff, T. & Bindereif, A. (1993). Conformational changes of U6 RNA during the spliceosome cycle: an intramolecular helix is essential both for initiating the U4–U6 interaction and for the first step of slicing. *Genes Dev.* **7**, 1377–1389.
- Nilsen, T. W. (2003). The spliceosome: the most complex macromolecular machine in the cell? *BioEssays*, **25**, 1147–1149.
- Staley, J. P. & Guthrie, C. (1998). Mechanical devices of the spliceosome: motors, clocks, springs, and things. *Cell*, **92**, 315–326.
- Brow, D. A. (2002). Allosteric cascade of spliceosome activation. *Annu. Rev. Genet.* **36**, 333–360.
- Achsel, T., Brahms, H., Kastner, B., Bachi, A., Wilm, M. & Lührmann, R. (1999). A doughnut-shaped heteromer of human Sm-like proteins binds to the 3'-end of U6 snRNA, thereby facilitating U4/U6 duplex formation *in vitro*. *EMBO J.* **18**, 5789–5802.
- Kambach, C., Walke, S., Young, R., Avis, J. M., de la Fortelle, E., Raker, V. A. *et al.* (1999). Crystal structures of two Sm protein complexes and their implications for the assembly of the spliceosomal snRNPs. *Cell*, **96**, 375–387.
- Beggs, J. D. (2005). Lsm proteins and RNA processing. *Biochem. Soc. Trans.* **33**, 433–438.
- Mayes, A. E., Verdone, L., Legrain, P. & Beggs, J. D. (1999). Characterization of Sm-like proteins in yeast and their association with U6 snRNA. *EMBO J.* **18**, 4321–4331.
- Vidal, V. P., Verdone, L., Mayes, A. E. & Beggs, J. D. (1999). Characterization of U6 snRNA–protein interactions. *RNA*, **5**, 1470–1481.
- Verdone, L., Galardi, S., Page, D. & Beggs, J. D. (2004). Lsm proteins promote regeneration of pre-mRNA splicing activity. *Curr. Biol.* **14**, 1487–1491.
- Shannon, K. W. & Guthrie, C. (1991). Suppressors of a U4 snRNA mutation define a novel U6 snRNP protein with RNA-binding motifs. *Genes Dev.* **5**, 773–785.
- Bell, M., Schreiner, S., Damianov, A., Reddy, R. & Bindereif, A. (2002). p110, a novel human U6 snRNP protein and U4/U6 snRNP recycling factor. *EMBO J.* **21**, 2724–2735.
- Raghunathan, P. L. & Guthrie, C. (1998). A spliceosomal recycling factor that reanneals U4 and U6 small nuclear ribonucleoprotein particles. *Science*, **279**, 857–860.
- Rader, S. D. & Guthrie, C. (2002). A conserved Lsm-interaction motif in Prp24 required for efficient U4/U6 di-snRNP formation. *RNA*, **8**, 1378–1392.
- Fromont-Racine, M., Mayes, A. E., Brunet-Simon, A., Rain, J. C., Colley, A., Dix, I. *et al.* (2000). Genome-wide protein interaction screens reveal functional networks involving Sm-like proteins. *Yeast*, **17**, 95–110.
- Jandrositz, A. & Guthrie, C. (1995). Evidence for a Prp24 binding site in U6 snRNA and in a putative intermediate in the annealing of U6 and U4 snRNAs. *EMBO J.* **14**, 820–832.
- Kwan, S. S. & Brow, D. A. (2005). The N- and C-terminal RNA recognition motifs of splicing factor

- Prp24 have distinct functions in U6 RNA binding. *RNA*, **11**, 1–13.
22. Ryan, D. E., Stevens, S. W. & Abelson, J. (2002). The 5' and 3' domains of yeast U6 snRNA: Lsm proteins facilitate binding of Prp24 protein to the U6 telomeric region. *RNA*, **8**, 1011–1033.
 23. Vidaver, R. M., Fortner, D. M., Loos-Austin, L. S. & Brow, D. A. (1999). Multiple functions of *Saccharomyces cerevisiae* splicing protein Prp24 in U6 RNA structural rearrangements. *Genetics*, **153**, 1205–1218.
 24. Brow, D. A. & Vidaver, R. M. (1995). An element in human U6 RNA destabilizes the U4/U6 spliceosomal RNA complex. *RNA*, **1**, 122–131.
 25. Puig, O., Caspary, F., Rigaut, G., Rutz, B., Bouveret, E., Bragado-Nilsson, E. *et al.* (2001). The tandem affinity purification (TAP) method: a general procedure for protein complex purification. *Methods*, **24**, 218–229.
 26. Stevens, S. W., Barta, I., Ge, H. Y., Moore, R. E., Young, M. K., Lee, T. D. & Abelson, J. (2001). Biochemical and genetic analyses of the U5, U6, and U4/U6×U5 small nuclear ribonucleoproteins from *Saccharomyces cerevisiae*. *RNA*, **7**, 1543–1553.
 27. Sheff, M. A. & Thorn, K. S. (2004). Optimized cassettes for fluorescent protein tagging in *Saccharomyces cerevisiae*. *Yeast*, **21**, 661–670.
 28. Moine, H., Ehresmann, B., Ehresmann, C. & Romby, P. (1997). Probing RNA structure and function in solution. In *RNA Structure and Function* (Simons, R. W. & Grundberg-Manago, M., eds), pp. 77–115, Cold Spring Harbor Laboratory Press, Cold Spring Harbor, NY.
 29. Ehresmann, C., Baudin, F., Mougel, M., Romby, P., Ebel, J. P. & Ehresmann, B. (1987). Probing the structure of RNAs in solution. *Nucl. Acids Res.* **15**, 9109–9128.
 30. Celander, D. W. & Cech, T. R. (1990). Iron(II)-ethylenediaminetetraacetic acid catalyzed cleavage of RNA and DNA oligonucleotides: similar reactivity toward single- and double-stranded forms. *Biochemistry*, **29**, 1355–1361.
 31. Urlaub, H., Hartmuth, K. & Lührmann, R. (2002). A two-tracked approach to analyze RNA–protein cross-linking sites in native, nonlabeled small nuclear ribonucleoprotein particles. *Methods*, **26**, 170–181.
 32. Ghetti, A., Company, M. & Abelson, J. (1995). Specificity of Prp24 binding to RNA: a role for Prp24 in the dynamic interaction of U4 and U6 snRNAs. *RNA*, **1**, 132–145.
 33. Reiter, N. J., Blad, H., Abildgaard, F. & Butcher, S. E. (2004). Dynamics in the U6 RNA intramolecular stem-loop: a base flipping conformational change. *Biochemistry*, **43**, 13739–13747.
 34. Fabrizio, P., McPheeters, D. S. & Abelson, J. (1989). *In vitro* assembly of yeast U6 snRNP: a functional assay. *Genes Dev.* **3**, 2137–2150.
 35. Mougin, A., Gottschalk, A., Fabrizio, P., Lührmann, R. & Branlant, C. (2002). Direct probing of RNA structure and RNA–protein interactions in purified HeLa cell's and yeast spliceosomal U4/U6.U5 tri-snRNP particles. *J. Mol. Biol.* **317**, 631–649.
 36. Zeiler, B. N. & Simons, R. W. (1998). Antisense RNA Structure and Function. In *RNA Structure and Function* (Simons, R. W. & Grundberg-Manago, M., eds), pp. 437–464, Cold Spring Harbor Laboratory Press, Cold Spring Harbor, NY.
 37. Lorsch, J. R. (2002). RNA chaperones exist and DEAD box proteins get a life. *Cell*, **109**, 797–800.
 38. Schroeder, R., Barta, A. & Semrad, K. (2004). Strategies for RNA folding and assembly. *Nature Rev. Mol. Cell Biol.* **5**, 908–919.
 39. Harada, F., Kato, N. & Nishimura, S. (1980). The nucleotide sequence of nuclear 4.8S RNA of mouse cells. *Biochem. Biophys. Res. Commun.* **95**, 1332–1340.
 40. Brow, D. A. & Guthrie, C. (1988). Spliceosomal RNA U6 is remarkably conserved from yeast to mammals. *Nature*, **334**, 213–218.
 41. Shukla, G. C. & Padgett, R. A. (2001). The intramolecular stem-loop structure of U6 snRNA can functionally replace the U6atac snRNA stem-loop. *RNA*, **7**, 94–105.
 42. Rinke, J., Appel, B., Digweed, M. & Lührmann, R. (1985). Localization of a base-paired interaction between small nuclear RNAs U4 and U6 in intact U4/U6 ribonucleoprotein particles by psoralen cross-linking. *J. Mol. Biol.* **185**, 721–731.
 43. Damianov, A., Schreiner, S. & Bindereif, A. (2004). Recycling of the U12-type spliceosome requires p110, a component of the U6atac snRNP. *Mol. Cell. Biol.* **24**, 1700–1708.
 44. Neubauer, G., Gottschalk, A., Fabrizio, P., Séraphin, B., Lührmann, R. & Mann, M. (1997). Identification of the proteins of the yeast U1 small nuclear ribonucleoprotein complex by mass spectrometry. *Proc. Natl Acad. Sci. USA*, **94**, 385–390.
 45. Shevchenko, A., Wilm, M., Vorm, O. & Mann, M. (1996). Mass spectrometric sequencing of proteins silver-stained polyacrylamide gels. *Anal. Chem.* **68**, 850–858.
 46. Hartmuth, K., Raker, V. A., Huber, J., Branlant, C. & Lührmann, R. (1999). An unusual chemical reactivity of Sm site adenosines strongly correlates with proper assembly of core U snRNP particles. *J. Mol. Biol.* **285**, 133–147.

Edited by D. E. Draper

(Received 4 November 2005; received in revised form 1 December 2005; accepted 3 December 2005)
Available online 20 December 2005